SNfactory Spectrophotometry Requirements Document

v0.2

Greg Aldering

Dec 4, 2000

1 Introduction

The baseline requirement for spectrophotometry for the SNfactory is an internally consistent extra-atmospheric flux calibration with systematic accuracy better than 1% under photometric conditions and better than 3% under non-photometric conditions. A knowledge of the flux calibration error on an internally consistent system is also required. A derived requirement is knowledge of whether conditions are photometric or non-photometric. The flux calibration systematics requirements apply over the spectral range where the total system throughput is greater than 20% of peak (∼3500–10500Å), with the exception of the sharp atmospheric O_2 bands (6900Å and 7600Å).

The components necessary to determine the flux calibration include:

$$
\begin{aligned}
t &= \text{time} \\
\lambda &= \text{wavelength} \\
X &= \text{airmass} \\
k(\lambda, t, X) &= \text{atmospheric extinction, as a function of } \lambda, t, X. \\
\phi(\lambda, t) &= \text{telescope throughput, as a function of } \lambda, t. \\
\xi(\lambda, t) &= \text{instrument throughput, as a function of } \lambda, t. \\
D(\lambda, t) &= \text{detector quantum efficiency, as a function of } \lambda, t. \\
S(\lambda) &= \text{intrinsic standard star spectrum, as a function of } \lambda. \\
s(\lambda, t, X) &= \text{observed standard star spectrum, as a function of } \lambda, t, X. \\
F(\lambda) &= \text{intrinsic field star spectrum, as a function of } \lambda. \\
f(\lambda, t, X) &= \text{observed field star spectrum, as a function of } \lambda, t, X.
\end{aligned}
$$

$S(\lambda)$ is given by published spectrophotometry of standard stars. It is possible that these published results contain systematic errors which exceed the desired SNfactory spectrophotometry absolute calibration budget. At this stage nothing can be done about this, thus only an internally consistent calibration budget is specified.

Atmospheric extinction can be decomposed into contributions from Rayleigh scattering, aerosol scattering, ozone absorption, molecular oxygen absorption, water absorption, and water scattering. None of these components can be considered constant, but a great deal is known about the typical spectral and temporal behavior of these components from calculations and monitoring. According to the GONG site survey (Hill, *et al.*1994), the extinction at Mauna Kea is among the lowest and most stable of any astronomical site. The average optical extinction

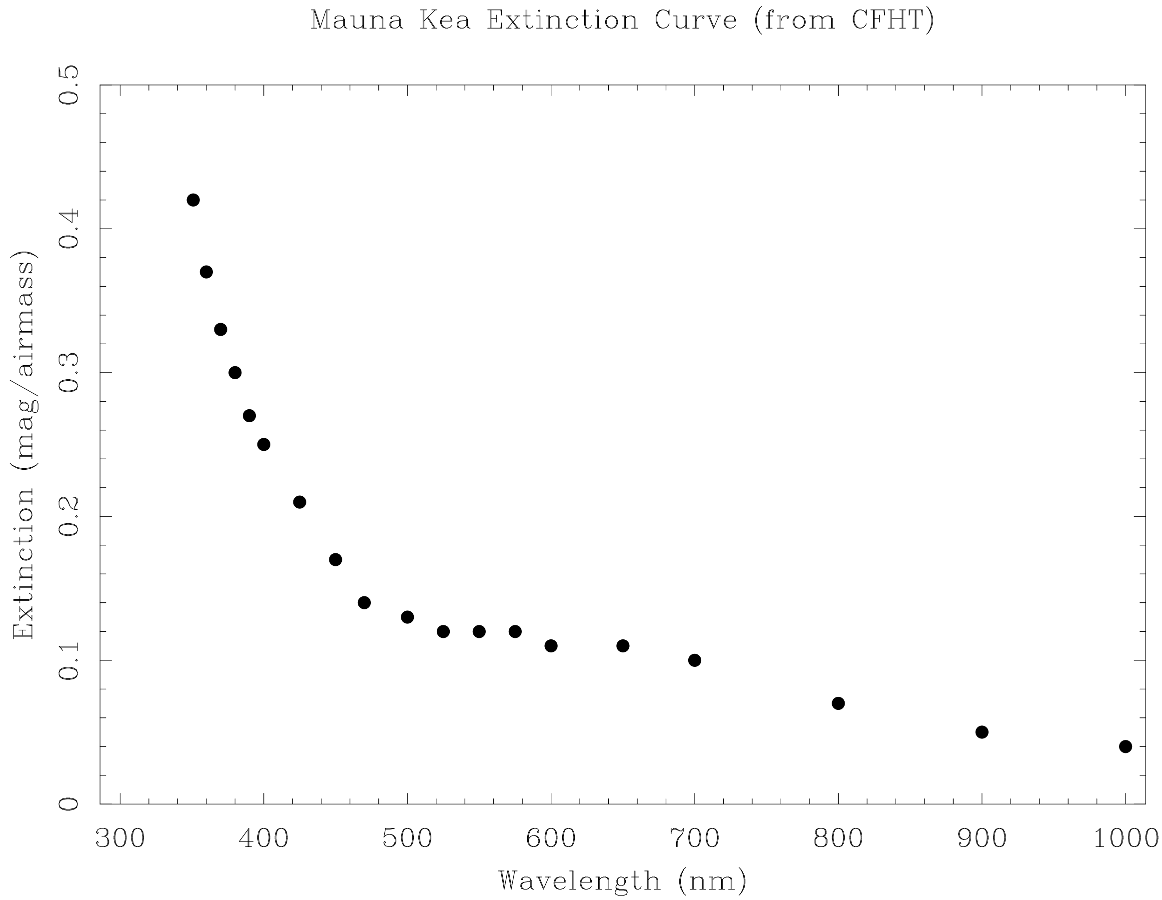

Figure 1: The extinction, in magnitudes per airmass, typical of Mauna Kea.

on clear days is 0.074, with a dispersion of only 0.015. The power spectrum of transmission variations measured by GONG during clear days follows the relation

$$(\Delta I/I_o)^2 = (\nu/10^{-6.80}Hz)^{-1.50} \tag{1}$$

where ν is the time frequency in Hz. This implies variations of 0.4% on timescales of one hour and variations of 1.7% over the course of a night. At La Silla, Burki, *et al.*, 1995 found that the total U-band extinction is correlated over a period of several days and that over one night the autocorrelation drops by only 5% (implying a typical 2.2% variation in extinction). These data indicate that ∼1% extinction variations can be expected over the course of a clear night, even at the best astronomical sites.

A closer examination of the following extinction components is needed to help clarify the source and spectral characteristics of such extinction variations:

Rayleigh scattering: Extinction due to Rayleigh scattering, k_R, is known to follow $a_R\lambda^{-4+x}$, where $x \sim 0.04$ is a very small correction to the canonical law. Rayleigh scattering dominates the extinction at most wavelengths under photometric conditions. a_R depends on the molecular scale height (roughly 8 km) which depends on altitude, and on weakly varying parameters like temperature, T, and pressure, P.

Aerosols: Extinction due to aerosol scattering, k_a, is generally the second greatest contributor. k_a is often parameterized as $a_a\lambda^\gamma$ (Ångstrom 1961). γ can vary widely, as shown in Fig. 2,

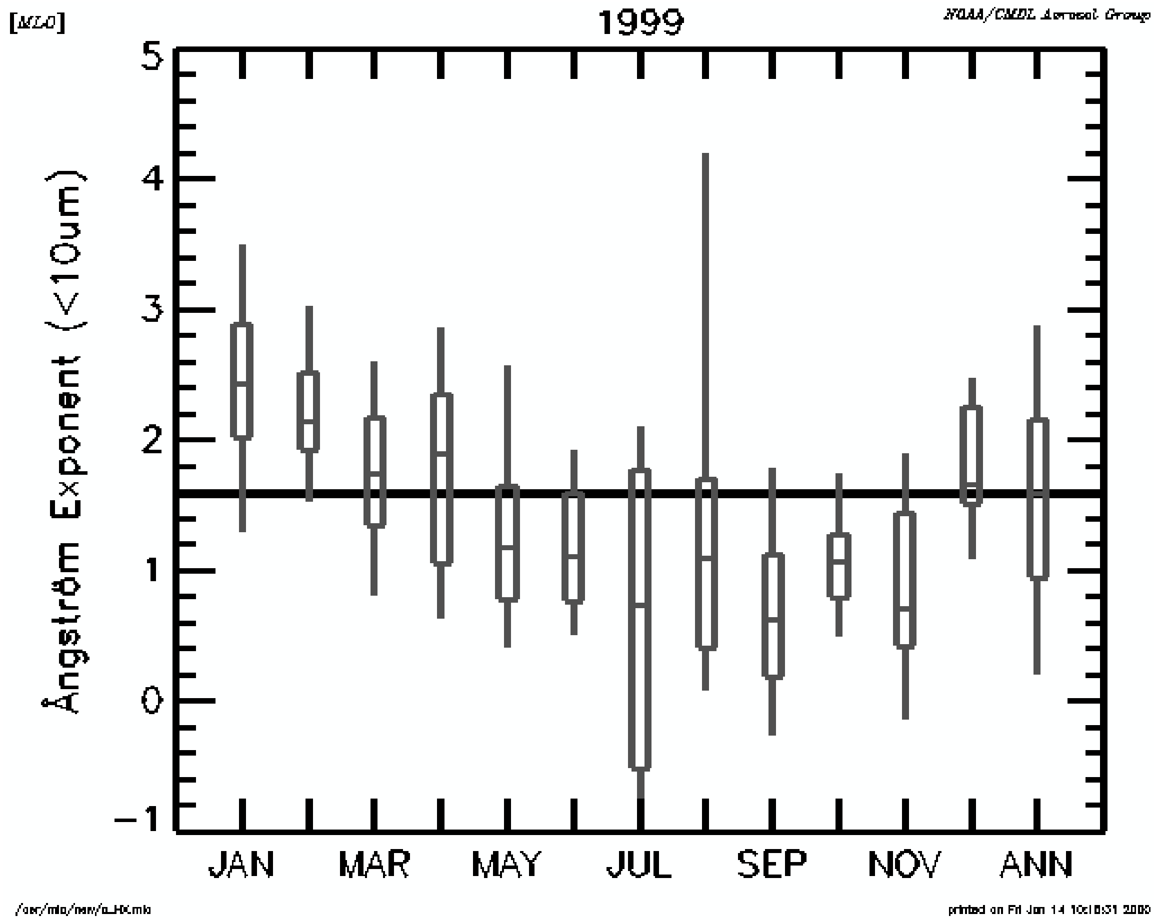

Figure 2: The variation in the Ångstrom aerosol extinction parameter, γ, measured over Mauna Loa in 1999. The central bar is the median, the boxes define the 25—75% range, and the outer whiskers denote the 5—95% range. Note that the Ångstrom exponent in this graph is equal to $-\gamma$. (From wwwsrv.cmdl.noaa.gov/aero/net/mlo/datacheck_mlo.html.)

using observations from Mauna Loa. γ depends on the particle size distribution of the aerosols, which shows variation with the source of a given mass of air and can change appreciably after significant volcanic explosions. Burki *et al.*1995 determined $\gamma = -1.39$ for La Silla using nights of low extinction. My modeling of the Mauna Kea extinction curve using libRadtrans indicates that a simple power law is inadequate to describe the aerosol scattering at that site. The aerosols on Mauna Kea are likely a mix of sea salt and volcanic dust from the summit and/or nearly islands ("vog," as it is known in Hawaii). The strong temperature inversion layer below the summit helps to keep a significant fraction of aerosols below the summit. Scattering (but not absorption) by suspended water droplets is generally included in the aerosol scattering budget.

Water vapor and ice: The extinction due to absorption by water vapor or clouds, $k_{H_2O,a}$ is generally absent or weak weak expect at a few wavelength intervals in the red. The night time scale height for H_2O is roughly 1 km. CSO monitoring indicates that $k_{H_2O,a}$ easily varies by factors of 2 over a few days (outer quartiles at 1.7 and 5.9 mm of water), and by several tens of a percent during a night on Mauna Kea (see Figs. 3 and 4). $k_{H_2O,s}$ only need be considered when clouds are present. It will be very time-variable as clouds pass through the field of view.

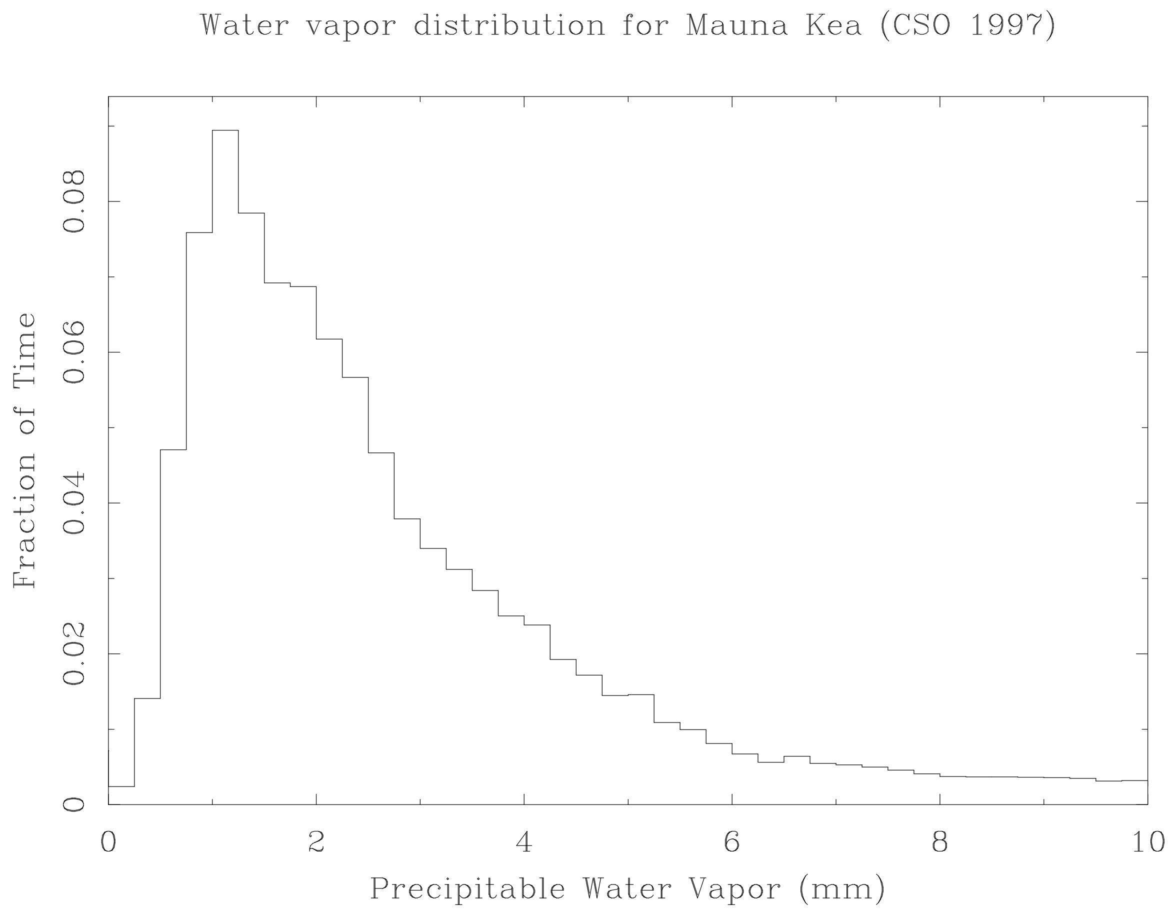

Figure 3: The frequency distribution of water vapor typical of Mauna Kea.

$k_{H_2O,s}$ is spectrally neutral according to theory due to the large number of random scatters in large water droplets or ice crystals.
Oxygen: Extinction due to ozone absorption, k_{O_3}, sets the UV limit for terrestrial observations, but is generally smaller than Rayleigh scattering over most of the optical spectrum. k_{O_3} has a spectral shape which is well known, but it's amplitude has seasonal variations and it is also reported to vary on timescales of hours (Hayes & Latham 1975). Daily O_3 observations covering 1966—2000 from Mauna Loa have a dispersion of 7%, with peak-to-peak variations of 36% (see www.cmdl.noaa.gov/dobson). A histogram of daily Mauna Loa ozone column values is shown in Fig 5. O_2 also produces absorption, k_{O_2}, which results in the A and B band absorption features. These are strong but narrow, and their shape is well known.

It is generally assumed that extinction sources follow the Beers-Lambert relation:

$$I_{obs} = I_{true} e^{-kX} \tag{2}$$

so the relation between the true spectrum of a star, $S(\lambda)$, and its observed spectrum, $s(\lambda, t, X)$ is given by:

$$s(\lambda, t, X) = \phi(\lambda, t)\xi(\lambda, t)D_S(\lambda, t)S(\lambda)\ exp[-X \sum_i^5 k_i(\lambda, t)] \tag{3}$$

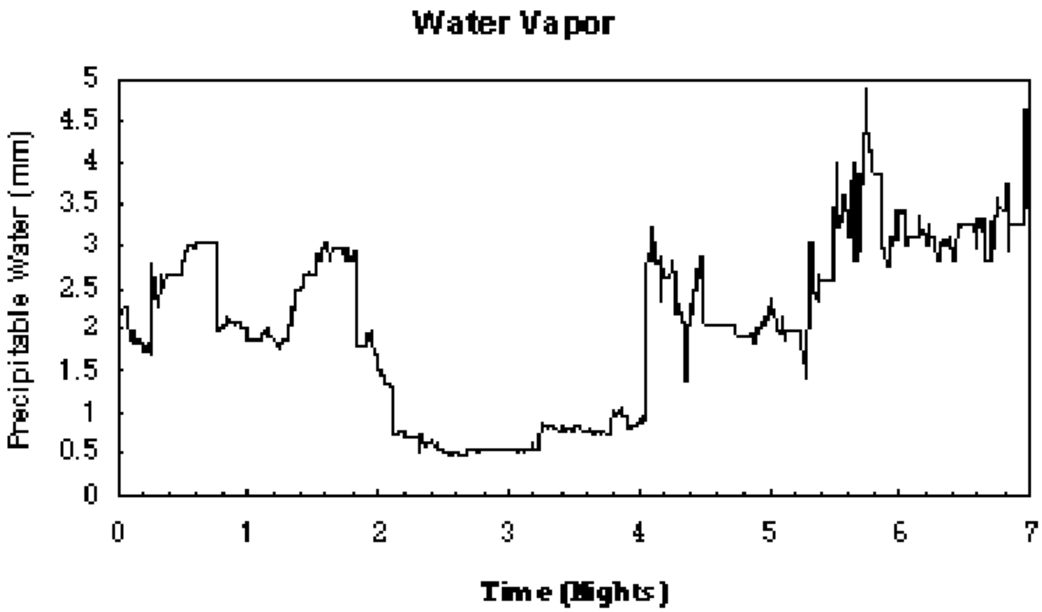

Figure 4: Representative Mauna Kea water vapor monitor readings, from CSO.

Exceptions include k_{O_2}, which goes as $X^{0.55}$, but this contribution can be easily determined from spectroscopy since it is so spectrally isolated. Assuming that the Beers-Lambert relation holds, the total extinction can be written as:

$$\begin{aligned} k(\lambda,t) &= k_R(\lambda) + k_a(\lambda) + k_{O_3}(\lambda) + k_{H_2O,a}(\lambda) + k_{H_2O,s}(\lambda) + k_{O_2}(\lambda) \\ &= a_R(t)\lambda^{-4+x} + a_a(t)\lambda^{\gamma} + a_{O_3}(t)\tau_{O_3}(\lambda) + a_{H_2O}(t)\tau_{H_2O}(\lambda) + a_{cld}\tau_{cld}(\lambda)) + a_{O_2}(t)\tau_{O_2}(\lambda) \end{aligned} \tag{4}$$

The functions $\tau_i(\lambda)$ represent the spectral properties of those extinction terms which are somewhat complicated, but which are known from external measurements. Note here I have separated the H_2O into a "normal" component which includes only absorption, and a "cloud" component. The scattering due to water vapor is not included in the "normal" component since it is is already accounted for in the aerosol-scattering term. The "cloud" term accounts for scattering by water and ice in clouds. τ_{cld} can change slightly depending on the ice/water fraction of the clouds, and further work is needed to characterize such changes. Additional absorption by water vapor in clouds is accounted for in the above scheme by the "normal" water component.

2 Extinction Correction under Photometric Conditions

When conditions are photometric, k is isotropic on the sky and has no time dependence. In this case $k(\lambda) = \sum_i^5 k_i(\lambda)$ can be solved for in Eqn. 2 by observing the spectrum, $s(\lambda, t, X)$, of at least two stars with known intrinsic spectrum, $S(\lambda)$. This statement implicitly assumes that the combined response of the telescope, instrumentation, and detector, given by:

$$C(\lambda,t) = \phi(\lambda,t)\xi(\lambda,t)D_S(\lambda,t) \tag{5}$$

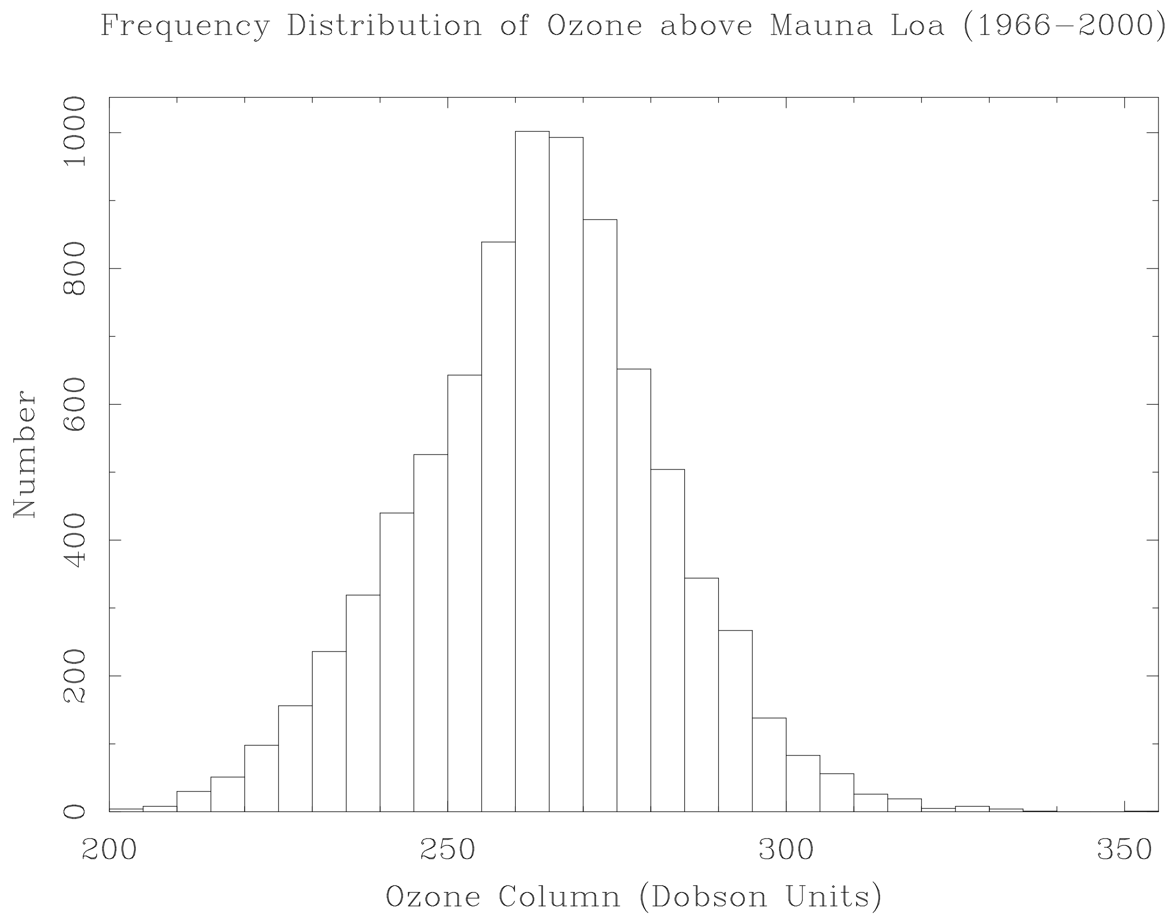

Figure 5: Histogram of Ozone over Mauna Loa, measured in Dobson units. Values are based on daily observations since 1966.

is constant in time. That is, it is assumed that $C(\lambda, t) = \overline{C}(\lambda)$, an issue which will be discussed below.

If $k(\lambda)$ is solved for at each wavelength, it is not necessary to determine the individual $k_i(\lambda)$ values for each extinction component. However, if $k(\lambda)$ must be smoothed due to low S/N or other reasons, then the relative contributions of the smooth (k_R, k_a, k_{O_3},$k_{H_2O,s}$) and structured ($k_{H_2O,a}$, k_{O_2}) components must be determined separately. Most reduction methods do this in an approximate way by only separating $k_{H_2O,a}$ and k_{O_2} at wavelengths were they are very large, and including spectral regions where they are not so strong in the calculation of the smooth component.

It will be useful to verify the above parameterization of k by decomposition of the SNfactory observations of spectrophotometric standards. This is tractable because the relative contributions of the various components vary with wavelength. Table 1 gives the relative contributions to the total extinction (mostly from La Silla); several key wavelengths at which a given atmospheric component will be most easily separable have extinction values indicated in bold.

Table 1 is also useful for identifying the extinction components which must be well-determined to provide better than 1% flux calibration. For instance, at most wavelengths k_R dominates and must be well-determined. Fortunately the behavior of $k_R(\lambda)$ is well known. k_a must be

Table 1: Extinction components per airmass at various wavelengths

λ	Rayleigh Scattering	Aerosol Scattering	Ozone Absorption	Water Absorption	O2 Absorption
3460	0.500	0.049	0.020	0.000	0.000
4000	**0.275**	0.041	0.000	0.000	0.000
5800	0.062	0.025	**0.023**	0.000	0.000
7600	0.021	0.017	0.002	0.000	**0.6**
8500	0.013	**0.015**	0.000	0.000	0.000
9300	0.009	0.013	0.000	**0.35**	0.000

determined to better than 10% (meaning constraints on both a_a and γ), while the amplitude a_{O_3} can be uncertain by 20%, before these sources cause any appreciable error. H_2O and O_2 must be determined very well (1%), but only at certain wavelengths where they are well isolated from the other components. A great advantage over existing work in this area is the large simultaneous wavelength coverage the SNfactory spectrograph will provide.

3 Extinction Correction under Non-Photometric Conditions

Two levels of non-photometric conditions can be defined:
Mildly non-photometric conditions are defined to occur when k is neither isotropic nor time invariant, but before the formation of any visible clouds. These conditions can occur for a number of reasons, most notably a transition from one weather system to another during which the aerosol content and composition, water content, temperature, and pressure are changing. (Note that the arrival of a new weather system changes temperature and pressure, which should therefore be routinely monitored as a clue that conditions may be non-photometric.) These conditions can also occur due to sinking of the aerosol layer (whose scale-height is typically only $\sim$1.5 km), and to a lesser degree the molecular layer (having an 8 km scale-height), during the night as the atmosphere cools.

Strongly non-photometric conditions are defined to occur whenever clouds of any kind are present. Since efficiency decreases quickly with cloud optical depth, the only situation under which fruitful observations might proceed is for thin cirrus clouds. In this situation, the scattering properties of clouds enter into the extinction through $k_{H_2O,s}$. As mentioned before, $k_{H_2O,s}$ is fairly gray (spectrally neutral).

Under mildly non-photometric conditions where temporal and spatial variations in k consist of large pockets of air, as with different weather systems, then the observations of spectrophotometric standard stars close in time and sky location to the observation of program objects may allow localized correction for extinction. Unfortunately, the accuracy of this approach is difficult to verify, since the location and temporal variations in k are not known *a priori*. With sufficient observations, trends in the standard star observations can be examined for evidence of smooth changes or an isolated transition in time or sky location. Only under these very simple situations can calibration exclusively from spectrophotometric standards hope to be sufficiently accurate.

Under strongly non-photometric conditions, observations of spectrophotometric standards is only of value of determining the relation between $k_{H_2O,a}$ and $k_{H_2O,s}$. Therefore, additional methods are needed in order for useful observations to be obtained under non-photometric conditions.

3.1 The role of a parallel imager

With the advent of CCD's, imaging follow-up of variable events such as supernovae has exploited the fact that over small fields of view non-photometric conditions tend to uniformly depress the flux from all objects in the field. Thus, non-variable objects in the field can be used as comparison objects, and once the brightness of such comparison objects is determined under photometric conditions, the relative brightness between the target object and comparison objects can be converted to an absolute flux. There are potential problems with this approach, namely the issues of whether the non-photometric conditions really are constant over a field, and whether the non-photometric conditions have a reasonably neutral spectrum so that the scaling does not depend on the spectrum of the comparison stars. The constancy of the non-photometric conditions across a field can be determined directly by comparing the variation in scaling determined using field stars observed during both photometric and non-photometric conditions. Thus, this uncertainty can be built directly into the error budget. For long exposures, a range of cloud patterns should be swept across the field of view, so most variations should be slowly varying across the field.

Most SNfactory supernova fields will be visited many times, and conditions can be expected to be photometric for some fraction of those visits. In particular, the visit during which a final reference spectrum is obtained can be chosen to occur during photometric conditions since it is not time-critical.

The imager will observe many stars surrounding each supernova. The intrinsic spectrum, $F(\lambda)$ of these stars is unknown and some fraction of them may be variable. The observation of star n, $f_n(\lambda_i, t, \alpha, \delta)$ can be presented as

$$f_n(\lambda_i, t, \alpha, \delta) = \int_0^{\infty} \int_t^{t+\Delta t} \phi(\lambda, t)\xi_{\lambda_i}(\lambda_i, t) D_I(\lambda, t) F_n(\lambda)\ exp[-X \sum_i^5 k_i(\lambda, t, \alpha, \delta)] d\lambda dt \qquad (6)$$

Where the imager instrument response, $\xi_{\lambda_i}(\lambda, t)$, is dominated by the response of a chosen filter, denoted by its central wavelength, λ_i. Since parallel imaging is only of value for photometric corrections of observations are obtained a precisely the same time as the spectroscopy, we assume that the interval t to $t + \Delta t$ is identical for both instruments and use t_j to label the observation at epoch j. This necessity leads to a derived requirement for common or synchronized shutters for the spectrograph and imager.

Assuming that the extinction is constant over a very small patch of sky surrounding the supernova and observed by the imager, and using the index x_k to label the field, one can write:

$$f_{n,\lambda_i,t_j,x_k} = f_{n,\lambda_i,t_j}(\alpha, \delta) \qquad (7)$$

Thus, for each star in a field the variation at a given wavelength during the course of j epochs is mapped out. Since some observations are obtained during photometric conditions, the absolute brightness of each star can be determined and subtracted to give the absolute variation:

$$\Delta f_{n,\lambda_i,t_j,x_k} = f_{n,\lambda_i,t_j,x_k} - f_{n,\lambda_i,x_k,corr} \qquad (8)$$

where *corr* denotes a flux corrected for extinction under photometric conditions. The measurements for all the stars observed in one image can be combined, to give:

$$\overline{\Delta f}_{\lambda_i,t_j,x_k} = \frac{1}{N}\sum_{n=1}^{N} \Delta f_{n,\lambda_i,t_j,x_k} \tag{9}$$

Clearly these values of $\overline{\Delta f}_{\lambda_i,t_j,x_k}$ provide some indication of the extinction variations over the wavelength span of each filter, and for a set of wavelengths should give some information on the extinction which applied to the contemporaneous and nearly co-spatial supernova observation.

However, there are two problems here. First, note that without explicit knowledge of the λ-dependencies of the other terms in the integral of Eqn 6, $f_{n,\lambda_i,corr}$ can not be calculated using $\sum_{i=1}^{5} k_i(\lambda)$ determined from spectrophotometric standard star observations. Instead each field, x_k, would have to be followed as a function of airmass on a photometric night so that $f_{n,\lambda_i,corr}$ on the instrumental system of the SNfactory imager could be determined for each star in that field. Such observations could be done quite easily, but at some loss of observing efficiency on photometric nights.

Second, with a single filter, only the average extinction correction over one wavelength interval is being measured at the time of the supernova observation. Given the earlier discussion showing that extinction has multiple components which do not scale together, such a measurement could only provide an average correction for the portion of the spectrum covered by the imager filter. Extrapolating to other filters would be difficult, but not necessarily impossible. For instance, in the case of increased water vapor due to incipient cirrus, one could imagine monitoring a water absorption band to estimate the column of water. The scattering component due to water will only become gray once clouds actually form since multiple scattering is required, however, by spectrally monitoring a standard star under such conditions, a mapping between the water vapor absorption and the extinction should be found and used for correction purposes. (As discussed earlier, water scattering depends somewhat on whether water is in ice or liquid form, and on the circumstances of ice formation. Thus, any such relation would have an associated uncertainty whose expected size is not known at present.) Similarly, changes in aerosol content can be important contributors to non-photometric conditions and one could imagine monitoring one bandpass to detect changes Δa_a, in the aerosol content if water vapor and other contributors were stable. Of course k_a depends on a_a and γ, so it would be necessary to assume a value of γ in order to extrapolate to other wavelengths. A typical value (and dispersion) for γ would be known from spectrophotometric standards observed under photometric conditions, however, Fig. 2 shows that this parameter isn't necessarily that stable. Knowledge of γ to ± 0.2 is sufficient to keep the calibration uncertainty below about 1%, for typical k_a.

Since extinction correction using monitoring one one wavelength is not necessarily sufficient, a solution for this and the field-star calibration problem will now be addressed.

3.2 Multicolor field-star monitoring

One might imagine simply expanding the above approach to include multiple filters. Since the observations must be taken simultaneously with spectroscopic observations, an imager would have to monitor different stars in a field using a single multicolor filter (e.g., a series of adjacent filters close to the focal plane). By covering the entire optical spectrum with filters, one would obtain the correct mean scaling for each portion of the simultaneous spectroscopic observations. However, even such full-coverage multicolor monitoring will not provide sufficient information to perfectly remove extinction since the different extinction components do not vary together. The uncertainty in this approach is difficult to predict because it depends on details of how much different extinction components can vary. In regions unaffected by water absorption, this approach might work rather well.

Table 1 and the previous discussion suggests a means of breaking the degeneracy amongst extinction components present in single-band or even full-coverage multicolor monitoring under non-photometric conditions. Namely, if $\overline{\Delta f}_{\lambda_i,t_j,x_k}$ is determined at wavelengths where each extinction component dominates, the parameterization of Eqn 4 could be used to determine the correct extinction to apply to the spectroscopic observations. Monitoring would have to occur at all λ_i at the same time in order to account for variations of all the extinction components. The parameters to be determined are $a_R(t_j)$,$a_a(t_j)$,$\gamma(t_j)$,$a_{O_3}(t_j)$, and $a_{H_20}(t_j)$. It is probable that a_{O_2} can still be determined using spectrophotometric standard star observations, even under non-photometric conditions, so it is not included here. Methods of this type are routinely used in remote sensing experiments.

If the instrument response is assumed to be constant, an observation taken with the imager in filter λ_i, at time t_j in field x_k can be described by:

$$f_{n,\lambda_i,t_j,x_k} = \int_0^\infty \phi(\lambda)\xi_{\lambda_i}(\lambda)D_I(\lambda)F_{n,x_k}(\lambda)\ exp[-X\sum_{i=1}^{5} k_i(\lambda,t,\alpha,\delta)]d\lambda \tag{10}$$

The extinction term can be decomposed into its various components

$$\sum_{i=1}^{5} k_i(\lambda,t,\alpha,\delta) = a_{R,t_j}\lambda^{-4+x} + a_{a,t_j}\lambda^\gamma + a_{O_3,t_j}\tau_{O_3}(\lambda) + a_{H_2O,t_j}\tau_{H_2O}(\lambda) + a_{cld,t_j}\tau_{cld}(\lambda) \tag{11}$$

giving

$$f_{n,\lambda_i,t_j,x_k} = \int_0^\infty C_{\lambda_i}(\lambda)F_{n,x_k}(\lambda)\ e^{[-X(a_{R,t_j}\lambda^{-4+x}+a_{a,t_j}\lambda^\gamma+a_{O_3,t_j}\tau_{O_3}(\lambda)+a_{H_2O,t_j}\tau_{H_2O}(\lambda)+a_{cld,t_j}\tau_{cld}(\lambda))]}d\lambda \tag{12}$$

In order to solve for the amplitudes of the various extinction components, the above equation can be linearized by expanding the extinction terms in the exponential about the mean extinction—airmass product, $< X\tau >$, in the given filter, e.g.,

$$f_{n,\lambda_i,t_j,x_k} \sim e^{-\langle X\tau\rangle} \int_0^\infty C_{\lambda_i}(\lambda)F_{n,x_k}(\lambda) \\ [1 + \langle X\tau\rangle - X\,(a_{R,t_j}\lambda^{-4+x} - a_{a,t_j}\lambda^\gamma - a_{O_3,t_j}\tau_{O_3}(\lambda) - a_{H_2O,t_j}\tau_{H_2O}(\lambda) - a_{cld,t_j}\tau_{cld}(\lambda))]d\lambda \tag{13}$$

$$
\begin{aligned}
f_{n,\lambda_i,t_j,x_k} \sim\ & e^{-\langle X\tau\rangle}(1+\langle X\tau\rangle) && V_{o,\lambda_i,n,x_k} \\
&+ e^{-\langle X\tau\rangle}X && a_{R,t_j,x_k}V_{R,\lambda_i,n,x_k} \\
&+ e^{-\langle X\tau\rangle}X && a_{a,t_j,x_k}V_{a,\lambda_i,n,x_k}(\gamma(t_j,x_k)) \\
&+ e^{-\langle X\tau\rangle}X && a_{O_3,t_j,x_k}V_{O_3,\lambda_i,n,x_k} \\
&+ e^{-\langle X\tau\rangle}X && a_{H_2O,t_j,x_k}V_{H_2O,\lambda_i,n,x_k} \\
&+ e^{-\langle X\tau\rangle}X && a_{cld,t_j,x_k}V_{cld,\lambda_i,n,x_k}
\end{aligned} \tag{14}
$$

Where

$$
V_{o,\lambda_i,n,x_k} = \int_0^\infty C_{\lambda_i}(\lambda)F_{n,x_k}(\lambda)d\lambda, \tag{15}
$$

$$
V_{R,\lambda_i,n,x_k} = \int_0^\infty C_{\lambda_i}(\lambda)F_{n,x_k}(\lambda)\lambda^{-4+x}d\lambda, \tag{16}
$$

and likewise for the other extinction terms. This approximation should be good to better than 1% for typical extinction values. The key is that observations in all I filters must be taken simultaneously. Only in this case can the number of degrees of freedom possibly be greater than zero (and as shown below, it is also necessary that that the number of epochs be six or greater.

A set of nearly linear equations relates the observables, f_{n,λ_i,t_j,x_k}, to the unknown a's and V's. The equations have a slight non-linearity due to the additional unknown γ's which effects the V_{a,n,λ_i}'s. It is almost certain that a_R, a_a, and γ will be correlated, but if the extinction correction so obtained is good, then this is not an issue. Of course the full correlation must be included in the calculations of the uncertainties. The number of observables are the fluxes in I filters, in K fields, of the N_K stars, for J_K epochs.

$$
N_{obs} = \sum_{filters}^{I} \sum_{fields}^{K} \sum_{epochs}^{J_K} \sum_{stars}^{N_K} \tag{17}
$$

(The values of the five a's and one γ determined for L of J photometric epochs from spectroscopy of spectrophotometric standards are not counted here): As an example, for equal numbers of stars and epochs in each field, $N_{obs} = IKJN = K(IJN)$.

The number of parameters is given by the five a's and one γ, to be determined at $J_K - L_K$ non-photometric epochs in K fields, plus the six V's for N_K stars in K fields for the I filters:

$$
N_{par} = 6\sum_{fields}^{K} \sum_{epochs}^{J_K-L_K} + 6\sum_{filters}^{I} \sum_{fields}^{K} \sum_{stars}^{N_K} \tag{18}
$$

Again, for equal numbers of stars and epochs in each field, $N_{par} = 6K(J-L) + 6IKN$. Note that for well-chosen filters, there will be just a few dominant V's for each measurement. In particular, for the water absorption filter all but one V can be zero for a properly-chosen filter. This reduces the number of unknowns. Likewise, it is reasonable to expect that a_R will not vary strongly during a night and so can be held fixed over the K fields observed on a given night, further reducing the number of free parameters.

To ensure that $N_{par} < N_{obs}$ we require $6K((J-L)+IN) < K(IJN)$. Since in this treatment each field is independent, the number of fields, K, cancels out. This can be reduced to $IN(J-6)-6(J-L) > 0$, which sets a *minimum* requirement that the number of epochs $J > 6$. Of course the number of degrees of freedom is not the entire story. As discussed earlier, decomposition of extinction into its various components is unlikely to succeed unless there is at least one well-positioned filter per component. Although additional stars help, a range of spectral types is required to provide substantially new information.

The above analysis shows that in principle the appropriate extinction as a function of wavelength can be determined from multicolor photometry of field stars taken *simultaneously* with spectrophotometric observations of a program object under non-photometric conditions. This method can be tested directly using such observations of spectrophotometric standard stars. Monte Carlo simulations, and up-to-date absorption spectral functions, are needed to validate the above analysis and to determine the best filters (central wavelengths, widths, and shapes) for the multicolor field-star monitoring.

4 The need to monitor system stability

So far it has been assumed that the $\phi(\lambda, t)$, $\xi_{\lambda_i}(t)$, and $D_I(\lambda, t)$ are constant over the entire one year period during which each supernova is observed. Moreover, even if parallel multicolor field-star observations are obtained to determine the extinction, the zero-point of the spectrograph, $\xi(\lambda, t)$, and the detector, $D_S(\lambda, t)$ must be known in order to obtain spectro*photometry* from the extinction-corrected spectra.

Before exploring a solution, the possible sources of zero-point change should be discussed. First, the telescope optics will collect dust and undergo cleaning and recoating. Dust accumulation alone can amount to 0.001 mag/day. The imaging filters, $\xi_{\lambda_i}(t)$ will have bandpasses that shift with temperature (and possibly humidity), and they will suffer degradation over time. The spectrograph optics should be fairly stable, however the dichroic beam-splitter can be expected to show changes with temperature, and to degrade over time. Finally, the $QE(\lambda)$ for the CCD detectors (D_S and D_I) will depend on cold-head temperature, and outgassing in the dewar will result in slow condensation of contaminants on the face of the detectors.

In the case of the spectrograph, regular observations of spectrophotometric standards on photometric nights will measure the product $C_S(\lambda, t) = \phi(\lambda, t)\xi(\lambda, t)D_S(\lambda, t)$ directly. Thus, if all sources of drift in the spectrograph zero-point are very slow, and photometric conditions occur sufficiently often, it may be possible to track $C_S(\lambda, t)$ for the spectrograph reasonably well. Sufficient standard stars will have to be observed to even ascertain whether or not conditions are photometric, unless there are other constraints on variations in $C_S(\lambda, t)$.

An approach using standard stars also might be considered for the imager. However, since the V's result from integrals over the spectral response of the imager and the unknown spectrum of the monitoring stars, shifts in filter wavelength — not just zero-point shifts — become an issue. In the parlance of ordinary photometry, this problem is one of a changing color term. In ordinary photometry, color terms are constrained by observation of stars having a wide range of spectra (colors), and such an approach might be possible here.

The careful reader will have noticed that with each new requirement needed to enable the use of non-photometric conditions, more and more of the observing time when conditions are photometric must be used for calibration. If calibration can not be done very quickly, observations described in this section will represent an undo burden. Moreover, the frequency of photometric conditions compared to expected changes in zero-points and color-terms is not yet known; if changes are fast compared to the frequency of photometric nights the calibration plan for using non-photometric nights may fail completely.

Young (1975) recommends that all precision photometry systems be monitored for stability using laboratory sources. This seems to be exactly what is required here. Since we are concerned with changes in both zero-points and color-terms, one solution would be to observe artificial stars produced by a suite of two or more stable lamps having different color temperature. The telescope response, $\phi(\lambda, t)$, is common to both the spectrograph and imager, and provided it is reasonably stable, the main outstanding calibration that is needed is that between the spectrograph and the imager.

4.1 Imager-to-Spectrograph scaling

In principle, a reference lamp observed simultaneously with the imager and the spectrograph will give the relative response of the spectrograph and imager. Imagine that the response of filters or spectral elements change only by scale factors, α_X, defined as follows:

$$C_I(\lambda, t_j) = \alpha_{C_I,t_j}\overline{C}_I(\lambda) \text{ (imager)} \tag{19}$$

$$C_S(\lambda, t_j) = \alpha_{C_S,t_j}\overline{C}_S(\lambda) \text{ (spectrograph)} \tag{20}$$

$$L(\lambda, t_j) = \alpha_{L,t_j}\overline{L}(\lambda), \tag{21}$$

where $L(\lambda)$ is the lamp spectrum. Simultaneous observations of the lamp with the imager and spectrograph at epoch t_1, $O_I(t_1)$ and $O_S(t_1)$ are given by:

$$O_I(t_1) = \int_0^\infty \alpha_{C_I,t_j}\overline{C}_I(\lambda)\alpha_{L,t_j}L(\lambda)d\lambda \tag{22}$$

$$O_S(t_1) = \alpha_{C_S,t_j}\overline{C}_S(\lambda_0)\alpha_{L,t_j}L(\lambda_0), \tag{23}$$

where λ_0 is arbitrary in this formulation. The ratio of these measurements yields:

$$\frac{O_I(t_1)}{O_S(t_1)} = \frac{\int_0^\infty \alpha_{C_I,t_j}\overline{C}_I(\lambda)\alpha_{L,t_j}L(\lambda)d\lambda}{\alpha_{C_S,t_j}\overline{C}_S(\lambda_0)\alpha_{L,t_j}L(\lambda_0)} = \omega_1\frac{\int_0^\infty \overline{C}_I(\lambda)L(\lambda)d\lambda}{L(\lambda_0)} \tag{24}$$

The values of ω_{t_j} thus track the relative sensitivity of the imager and spectrograph for any combination of imager filter and spectrograph wavelength, λ_0 (although it will be most sensible to compare at similar wavelengths, as will now be shown).

Of course it is likely that changes in the lamp spectrum will occur at different epochs unless care is taken to stabilize its response. How well must the lamp spectrum be stabilized? Following King (1952), the above integrals can be expanded as a Taylor series in derivatives of the lamp spectrum. The expansion is taken about the wavelength which is the 1st moment of the imager response (filter plus detector):

$$\lambda_0 = \mu_1 = \frac{\alpha_{C_I,t_j} \int_0^\infty \lambda \overline{C}_I(\lambda) d\lambda}{\alpha_{C_I,t_j} \int_0^\infty \overline{C}_I(\lambda) d\lambda} = \frac{\int_0^\infty \lambda \overline{C}_I(\lambda) d\lambda}{\int_0^\infty \overline{C}_I(\lambda) d\lambda} \tag{25}$$

(Note that λ_0 is immune to scaling changes in the imager response.)

The expansion given by King results in:

$$O_I(t_1) \approx \alpha_{C_I,t_j} \left(L(\lambda_0) \int_0^\infty \overline{C}_I(\lambda) d\lambda + \frac{dL(\lambda)}{d\lambda} \int_0^\infty (\lambda - \lambda_0) \overline{C}_I(\lambda) d\lambda + \frac{1}{2} \frac{d^2L(\lambda)}{d\lambda^2} \int_0^\infty (\lambda - \lambda_0)^2 \overline{C}_I(\lambda) d\lambda \right) \tag{26}$$

$$\approx \alpha_{C_I,t_j} \left(L(\lambda_0) \int_0^\infty \overline{C}_I(\lambda) d\lambda + \frac{1}{2} \frac{d^2L(\lambda)}{d\lambda^2} \int_0^\infty (\lambda - \lambda_0)^2 \overline{C}_I(\lambda) d\lambda \right) \tag{27}$$

$$\approx \tilde{\alpha}_{C_I,t_j} \left(L(\lambda_0) + \frac{1}{2} \mu_2^2 \left(\frac{d^2L(\lambda)}{d\lambda^2}_{|\lambda_0} \right) \right), \tag{28}$$

where μ_2 is the 2nd moment of the imager bandpass, and is defined in a manner analogous to μ_1. Note that the definition of λ_0 forces the 1st order term in the Taylor expansion to zero.

Now the earlier expression for the relative scaling of the imager and spectrograph can be rewritten as:

$$\frac{O_I(t_1)}{O_S(t_1)} = \tilde{\omega}_1 \frac{L(\lambda_0) + \frac{1}{2}\mu_2^2 \left(\frac{d^2L(\lambda)}{d\lambda^2)}_{|\lambda_0} \right)}{L(\lambda_0)} = \tilde{\omega}_1 \left(1 + \frac{1}{2}\mu_2^2 \left(\frac{1}{L(\lambda_0)} \frac{d^2L(\lambda)}{d\lambda^2)}_{|\lambda_0} \right) \right) \tag{29}$$

Here it is made clear that the observed flux ratio, $O_I(t_1)/O_S(t_1)$, tracks the relative response of the imager and spectrograph only if the normalized 2nd derivative of the lamp spectrum at the filter wavelength λ_0 is very small or the same from epoch to epoch. Therefore, a lamp with a linear spectrum (in photons), or a temperature-stabilized lamp is required. Since linear spectrum sources aren't available (to our knowledge!), the required temperature stability has been investigated. For a filter having $\mu_2 \sim 400$Å, a NIST-calibrated FEL lamp stabilized at a color temperature of $T = 2856 \pm 8K$ (see Fig. 6) is just sufficient to keep color errors below 0.5% across the entire optical spectrum (the most stringent constraint is for $\lambda_0 < 4000$Å). A warmer lamp, with $T \sim 5000K$, would have an even smaller sensitivity. The ability to track the relative response of the imager and the spectrograph leads to a derived requirement for a stabilized lamp, preferably having as small of a normalized 2nd derivative as possible so that the stability of μ_2 is not a factor.

4.2 Imager wavelength shifts and bandwidth changes

In the above discussion, a characteristic wavelength, λ_0, was defined for each imager channel. For all glass and interference filters the characteristic bandpass is dependent on the ambient

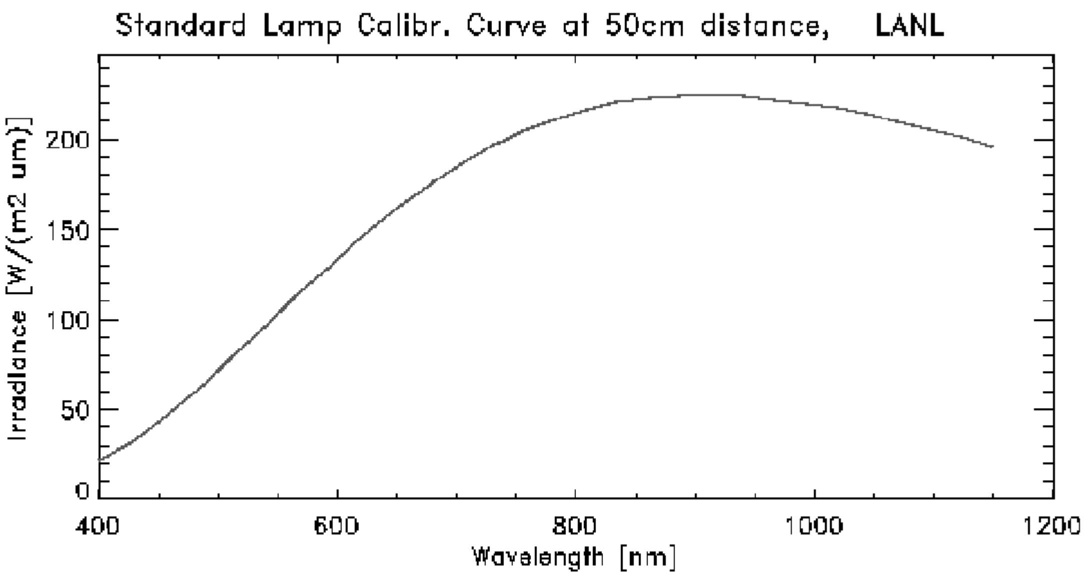

Figure 6: The spectrum of an NIST-calibrated FEL lamp. The lamp temperature is stable at $T = 2856 \pm 8K$. This stability is required to obtain a small, constant $\frac{1}{L(\lambda_0)} \frac{d^2L(\lambda)}{d\lambda^2)}_{|\lambda_0}$. It also allows completely internal relative flux calibration of the spectrograph good to 1%.

temperature. The wavelength response of the CCD can also change with operating temperature. The best solution for the latter problem is to stabilize the temperature to the requisite accuracy, as determined from laboratory tests. This leads to a derived requirement for laboratory tests of $dQE(\lambda, T)/dT$ for the CCD's, and temperature stabilized to the necessary accuracy (TBD).

The bandpass shifts for high-quality interference filters range from 0.015 nm/K to 0.025 nm/K across the optical. Colored glass filters have larger temperature coefficients, and so should be avoided for these purposes. Although the Mauna Kea site has good temperature stability, it seems sensible for the calibration procedure to be able to handle changes of $\pm 10\ K$. Filter temperature stabilization is possible, but presents a heat source in the imaging plane and thus may degrade the image quality. From Eqn. 23 we see that a shift in wavelength produces a term

$$\Delta O_I(t_1) = \tilde{\alpha}_{C_I,t_j} \frac{1}{L(\lambda_0)} \frac{dL(\lambda)}{d\lambda}_{|\lambda_0} \Delta\lambda_0 \tag{30}$$

For a NIST FEL lamp this amounts to no more than:

$$\Delta O_I(t_1) = \tilde{\alpha}_{C_I,t_j} 0.03\,\mathrm{nm}^{-1} \Delta\lambda_0 \tag{31}$$

and for the temperature coefficient of a high-quality interference filter this becomes:

$$\Delta O_I(t_1) = \tilde{\alpha}_{C_I,t_j} 0.03\,\mathrm{nm}^{-1}\, 0.025\mathrm{nm}/K\Delta T \tag{32}$$

$$= \tilde{\alpha}_{C_I,t_j} 0.00075\, K^{-1} \Delta T \tag{33}$$

Thus, a $\pm 10\ K$ temperature excursion can produce a calibration error of up to $\pm 0.75\%$, which is just at the level of being problematic. Fortunately, the filter temperature coefficient is only

0.015 nm/K in the blue, where the normalized derivative of the FEL lamp is largest, and so the expect error is more like $\pm 0.45\%$, which is acceptable.

Note that a wavelength shift for the imager will also change the V's, which must be stable over a period of 1 year. The effect on the V's will depend on the normalized slope of the star spectra. Thus, monitoring filter bandpass wavelengths and shapes should be chosen to give an imager response which is not effected by strong stellar absorption features. Unlike the case with the FEL lamp, different stars will present normalized derivatives with different signs, and so systematic errors in the V's could be small. This must be verified with simulations using realistic imager responses and stellar spectra.

A more proactive step would be to use lamps at two (or more) different operating temperatures to directly monitor the change in imager/spectrograph flux ratios as the normalized derivatives are changed. One lamp would have to be very stable for the reasons already cited. The normalized derivatives of the second lamp could be calibrated using the spectrograph observations of the stabilized lamp, and so they too would be known. It would be preferable to obtain a lamp temperature giving derivatives with opposite sign to a NIST FEL lamp. This requires a much hotter operative temperature, or perhaps a Cerenkov source such at that discussed by Young 1975. An alternative would be to place a gently sloping filter in front of the FEL lamp; drift in this filter would not be an issue since it's response would be calibrated using spectrograph observations of the lamp with and without the filter. Melles Griot sells "color temperature conversion filters" intended for just this purpose. Since O_I/O_S also depends on changes in μ_2, the filter width can be monitored independently of scaling and wavelength shift if a second color filter is added.

4.3 Location of photometric calibration sources

From a calibration point of view, it would be best if calibration lamps used to internally monitor the system were observed through the entire system, including the OTA. With a calibrated NIST FEL lamp, such observations would provide the correct wavelength-dependent flux calibration for the spectrograph, which is highly desirable both as an aid in data reduction and as a check on external wavelength-dependent flux calibration (within a scale factor) from spectrophotometric standard stars.

In this case, the telescope would have to directly view an artificial star constructed using a NIST FEL lamp and located on the dome. The standard procedure of illuminating a dome flat screen might work if a spectrally neutral screen material can be found. Of course in this case the absolute calibration of the NIST FEL lamp could not be exploited. Also, at this location, calibration observations would require that the telescope be open and pointed at the artificial star or screen. This may present operational difficulties, effecting when such calibration observations can be obtained. The advantage of this arrangement is that all the spectrograph and multicolor imaging observations can be obtained simultaneously with the multicolor filter in its regular observing position. No instrument modifications would be necessary since the normal observing arrangement would be utilized.

If operational difficulties — or problems implementing an adequate artificial star or dome flat screen — prevent use of a totally external lamp, the relative imager/spectrograph calibration can still be obtained internal to the SNfactory instrument. This would require a beam splitter to direct the already-required spectral flat lamp to send light to the imager. The multicolor filter in

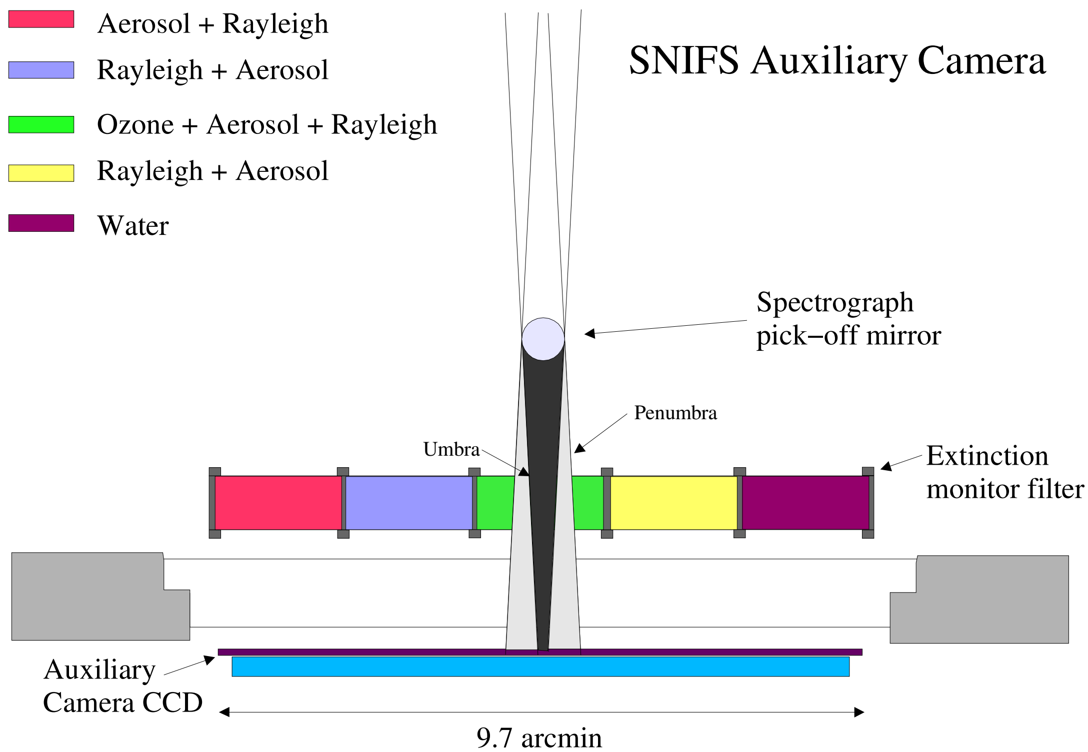

Figure 7: Possible layout for a multicolor extinction imaging filter.

the imager would have to be rotated in partial steps so that the beam-split light can be directed through each filter sequentially. Additional flat lamps or color temperature filters should then be added to the spectrograph calibration assembly.

Note that since a temperature stabilized lamp is a good choice for the spectrograph flat lamp, and since a beam-splitter is as simple as a mirror for the lamp pick-off mirror, it seems straightforward to implement the minimal internal flux calibration equipment within the SNfactory instrument. An external flux calibration module can then be pursued separately.

5 Multicolor imaging implementation

For a 2k×4k CCD with 15μm pixels on a 2.2-m f/10 telescope, the field is $6.1' \times 12.1'$. A 5-color filter (e.g., at wavelengths similar to those given in Table 1) would partition the field into $2.4' \times 6.1'$ regions. At the north Galactic pole about 6 stars are expected in a region this size down to $m_R = 19.5$. At R-band, the brightness of the faintest of these stars should be measurable to a few percent on a 2.2-m in a 300Å-wide filter in a 500 second exposure (the latter being typical of minimum spectroscopic exposures) for typical Mauna Kea seeing. Therefore, the surface density of useful stars is more than sufficient to overconstrain the series of equations needed to solve for temporal extinction variations.

6 Conclusion

A combination of observations of spectrophotometric standard stars and internal calibration should allow SNfactory calibration systematics to be kept below 1%. Reliance on only spectrophotometric standard stars will consume a non-negligible portion of observing time and is useful only under photometric conditions. We do not yet know the fraction of nights that are photometric to 1% on Mauna Kea, nor do we know how extensive spectrophotometric standard star observations must be to reliably establish a given night as photometric to 1%. Given these unknowns, and with an eye towards saving precious observing time, internal calibration should be provided to track sensitivity changes in the instrumentation.

Further observing time can be salvaged if non-photometric nights can be used. A method to determine the extinction correction to apply to the spectroscopy using simultaneous multicolor imaging of nearby field stars appears feasible. This method also requires an internal calibration capability utilizing a stable lamp. The internal calibration is better able to characterize the imager if a filter to modify the color-temperature is available. (Alternatively a very blue lamp would work.)

These, and related derived requirements include:

A) The ability to determine whether or not a given night or smaller interval of time is photometric is required.

B) On photometric nights (estimated 50% of total), spectrophotometric standard stars must be observed close in time and sky location to target supernovae so that correction for atmospheric extinction can be determined. (Number, airmasses, and spectral types TBD.)

C) The optical telescope assembly (OTA), instruments and their detectors must be stable over the course of one week, as sufficient observations of standard stars to constrain both atmospheric variations (non-photometric conditions) and instrumental variations will not be possible. (Limits on stability TBD, but expected to be $< 0.5\%$.) If these specifications can not be met and validated, accurate internal calibration must be provided. An internal calibration method, possibly exclusive of the OTA, is described in this document.

D) On non-photometric nights a mechanism to determine the spectral scaling needed to correct for non-photometric conditions is required. A suggested solution using simultaneous multicolor imaging of field stars surrounding monitored SNe is described in this document.

E) Laboratory tests of $dQE(\lambda, T)/dT$ for the imager CCD, and temperature stabilization of the CCD's to a TBD accuracy.

F) The ability to internally monitor imager wavelength shifts and bandpass widths is desirable. Lamps with additional color temperatures, or color temperature filters, could be used for this purpose. Such lamps would have to be observable with the imager and spectrograph simultaneously.

G) The imager and the spectrograph must have a common shutter, or synchronized shutters. This is required so that atmospheric and calibration conditions are identical for both instruments.

7 References

Ångstrom, A., 1961, "Technique of Determining the Turbidity of the Atmosphere," Tellus, Vol. 13, pp. 214-231.

Burki, G., Rufener, F., Burnel, M., Richard, C., Blecha, A, and Beatschi, P. 1995, "The atmospheric extinction at the E.S.O. La Silla observatory," A&AS, 112, 383.
Hayes, D. S., and Latham, D. W. 1975, "A Rediscussion of the Atmospheric Extinction and the Absolute Spectral-Energy Distribution of Vega," ApJ, 197, 593.
Hill, F., *et al.*1994, "The Global Oscillation Network Group Site Survey", Solar Physics.
King, I., 1952, "Effective Extinction Values in Wide-band Photometry", A.J., 57, 253.
Young, A. T. 1974, in "Methods of Experimental Physics: Volume 12-PartA, Optical and Infrared Astrophysics," ed. N. Carleton, Academic Press, New York.